Hindawi
Shock and Vibration
Volume 2023, Article ID 6604388, 13 pages
https://doi.org/10.1155/2023/6604388

Research Article

Study on the Influence Factors on Harvesting Capacity of a Piezoelectric Vibration Energy Harvesting System Covered on Curved Beam with Acoustic Black Hole

Miaoxia Xie, Fengwei Gao, Peng Zhang, Yuanqi Wei, Meijuan Tong, Yumin He, and Guanhai Yan

School of Mechanical and Electrical Engineering, Xi'an University of Architecture and Technology, Xi'an 710055, China

Correspondence should be addressed to Miaoxia Xie; x_m_xspace@163.com

Received 15 May 2023; Revised 13 November 2023; Accepted 24 November 2023; Published 4 December 2023

Academic Editor: Erkan Oterkus

The acoustic black hole (ABH) structures have been shown to have great potential for energy harvesting. Within an ABH, the bending wave velocity decreases rapidly and the phase accumulates, resulting in localised energy accumulation. It is very significant that the energy can be harvested and power can be supplied for microelectronic devices. How to improve energy harvesting capacity is a problem that needs to be solved. Previous research on energy harvesting capacity of straight beams and flat plates with ABH has yielded a wealth of results. However, in practical engineering, curved beams are also commonly found. Given the differences in structure, it is of practical significance to study the influence factors on harvesting capacity of the piezoelectric vibration energy harvesting system covered on curved beam with acoustic black hole. First, the vibration characteristics of curved beam with ABH are analysed by the finite element method and localised energy accumulation is observed. Then, energy harvesting capacity is studied by means of the electromechanical coupling model in FEA; it has been found that energy harvesting capacity is lower in high frequency. The reason of this problem is analysed and solved by dividing the size of the piezoelectric sheet in an array layout. Based on this, the influence of array layout of piezoelectric cells on the energy harvesting capacity of the system is focused on. In addition, the influence of resistance value, material property, and curvature of curved beam on the energy harvesting capacity is analysed. Some meaningful results are obtained. These results provide the guidance to the design and optimisation for an energy harvesting system covered on curved beam with ABH.

1. Introduction

In recent years, ABH structures have been widely investigated as an efficient technique for bending wave manipulation. ABH structures are such that the thickness of structures is changed as power law. If bending wave propagates in ABH, along with the thickness of the structure decreasing to zero, the wavelength is compressed, the wave velocity decreases, and the reflection does not occur at the location where thickness is zero, thus forming local energy accumulation [1–3]. With the deepening research of dynamics analysis theory for ABH [4, 5], ABH also shows great potential for vibration and noise control [6–15], energy harvesting [16–18], and bending wave manipulation [19–21]. With the help of pasting piezoelectric sensors, vibration energy is transferred into electrical energy and the purpose of energy harvesting is achieved [22].

Compared to the ABH effect in vibration and noise control and bending wave manipulation, the research on energy harvesting started late. Initially, Zhao et al. [16] covered five complete piezoelectric sensors in five ABH regions on a straight beam for energy harvesting, and the results of numerical simulation method showed that the energy conversion performance of ABH was better than that of uniform beam. Subsequently, Zhao [23] and others performed an experiment to verify the potential of ABH in energy harvesting. As the research continued, questions about how to optimise and enhance the energy harvesting

capacity of the ABH were considered. Ji et al. [17] designed an energy harvesting system with an array of piezoelectric sheets arranged in the ABH region to achieve enhanced harvested power. The reason for this treatment is that the wavelength of bending wave propagating in the structure is compressed as it approaches the ABH tip. At this point, when the size of the piezoelectric sheet is larger than half a wavelength, the energy conversion capacity of the ABH is severely weakened by the phase neutralisation of the anisotropic charges. Therefore, matching the size of the piezoelectric sheet to the wavelength variation is an effective remedy. Then, Zhang et al. [24] established the electromechanical coupling equations between the piezoelectric element and the ABH tapered straight beam under the premise of Timoshenko beam assumption. Also, Deng et al. [25] established a semianalytical model of energy harvesting about the ABH cantilevered straight beam by taking Gaussian function as the trial function in Rayleigh–Ritz method. The important influence of wavelength compression effect in the energy harvesting process was also verified by segmenting the piezoelectric sheet. Li et al. [26] designed a piezoelectric cantilever beam model equipped with an ABH structure and analyzed in detail the effects of piezoelectric sheet size and circuit type on the energy capture efficiency to provide a solution for the optimal design of the energy harvesting model. Qin et al. [27] adapted the power-law profile of ABH to the Eulerian exponential form on the basis of the ABH theory and applied it to a thin-plate structure, and through simulation and experimental methods, they verified that the new form of ABH structure has better voltage and power output than the power exponential form in the low frequency interval. The piezoelectric vibration energy harvester integrated with the beam of a bilateral periodic 1D ABH is proposed in reference [28]. The harvested energy performance of the structure is compared with that of the conventional ABH straight beam based on the finite element method and the experimental method, and the results show that the energy conversion capacity of the structure is about 10 times higher than that of the conventional model. The study in reference [29] shows that on the basis of piezoelectric energy mounting, higher output power can be obtained by arranging arrayed ABHs on the structure with better broadband characteristics compared to individual ABH features. Most of the research has focused on the application of the ABH effect to straight beams and flat plates [30–34]. However, various forms of curved beam and curved shell structures are widely used in fields such as aerospace and navigation. Therefore, it is of great engineering importance to analyse the application of the ABH effect on curved beam structures.

Unlike straight beams with ABH, the research on curved beam with ABH is complex due to the influence of the initial curvature. Annular beam and cylindrical curved shell structures with ABH used for vibration or acoustic control have been investigated [35–38], but the issue of applying curved beams with ABH to vibration energy harvesting has not been investigated in detail. In this paper, therefore, the curved beam with ABH is the main object of analysis, and the finite element method is used as the analysis method, with the ultimate goal of improving the energy harvesting capacity of piezoelectric vibration energy harvesting system covered on curved beam with ABH.

In Section 2, the energy accumulation theory of structures with ABH is introduced. In Section 3, the vibration response characteristics and energy accumulation effect of the curved beam with ABH are analysed based on the finite element harmonic response analysis. The energy harvesting capacity of piezoelectric vibration energy harvesting system covered on the curved beam with ABH is performed based on the piezoelectric coupling between the piezoelectric sheet and vibration of the curved beam with ABH. In Section 4, the wavelength compression phenomenon and considering its effect on energy harvesting is analysed. The effect of several key factors on the energy harvesting efficient is then specifically analysed. Conclusions are drawn in Section 5.

2. Energy Accumulation Theory of Structures with ABH

In 1988, Mironov [1] discovered a special phenomenon in variable-thickness plate structures, for bending waves propagating along the direction of decreasing thickness is no longer reflected at the position that thickness is zero (ideally), where the relationship between the wave number k and the amplitude A of the bending wave and the thickness of the structure satisfies as follows:

$$k = \left(\frac{3\rho\omega^2}{Eh^2(x)}\right)^{1/4}, \qquad A = A_0\left[\frac{h_0}{h(x)}\right]^{1/4}, \tag{1}$$

where ρ is the material density of the beam. E is Young's modulus of the beam. x is the coordinates of the plate along the direction of decreasing thickness. ω is the angular frequency. $h(x)$ is the thickness variation along the x axis. h_0 is the maximum thickness of the plate. A_0 is the amplitude of the bending wave in the position of maximum thickness. A sufficiently smooth variation in the thickness of the plate is required if the variation of wavelength over the variation in coordination of x axis is sufficiently small, then

$$\frac{1}{k^2}\frac{dk}{dx} \ll 1. \tag{2}$$

Combining the above equations yields

$$\frac{1}{2}\left(\frac{E}{3\rho\omega^2}\right)\frac{1}{\sqrt{h}}\frac{dh}{dx} \ll 1. \tag{3}$$

At this point, as shown in Figure 1, if the thickness of the plate varies in accordance with the power law, i.e.,

$$h(x) = \varepsilon x^m. \tag{4}$$

Substituting equation (4) into equation (3), then

$$\mathrm{m}x^{m-1} \ll 2\left(\frac{3\rho\omega^2}{E}\right)^{1/4}\frac{1}{\sqrt{\varepsilon}}x^{m/2}. \tag{5}$$

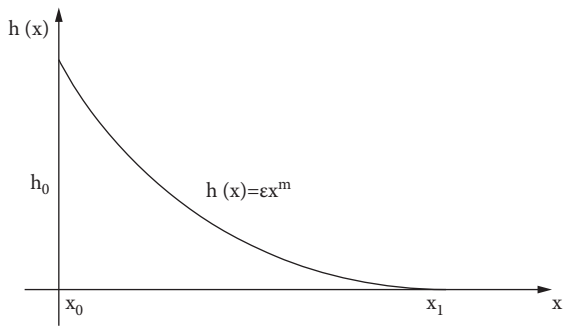

Figure 1: Outline of the ABH structure.

If the condition $m \geq 2$ is satisfied, furthermore, the group velocity c_1 and phase velocity c_2 of the bending wave are expressed as follow.

$$c_1 = \frac{\omega}{k} = \sqrt{\varepsilon}\left(\frac{E\omega^2}{3\rho}\right)^{1/4}, \quad c_2 = \frac{\partial\omega}{\partial k} = 2\sqrt{\varepsilon}\left(\frac{E\omega^2}{3\rho}\right)^{1/4}. \tag{6}$$

It can be found that as the wave number of the bending wave tends to infinity, c_1 and c_2 will tend to zero. Take T as time that the wave propagates from x_0 to x_1, then

$$T = \int_{x_0}^{x_1} \frac{dx}{c_2} = \frac{1}{2\sqrt{\varepsilon}}\left(\frac{3\rho}{E\omega^2}\right)^{1/4}\left|\ln\frac{x_1}{x_0}\right|. \tag{7}$$

Equation (7) shows that if $x_1 \longrightarrow 0$, $h(x) \longrightarrow 0$, the time that bending wave propagating to the tip of the structure is infinitely large, which means that the bending wave cannot reach the tip of the structure, and therefore no longer reflects. It results in a local vibration energy accumulation phenomenon. This theory also reveals that the ABH structure has the potential for efficient energy harvesting. Although the ABH effect is weakened in nonideal conditions (presence of truncated thickness), the ABH structure still performs better in terms of energy accumulation, compared to a uniform beam. This paper focus on analyzing the energy accumulation properties and energy harvesting capacity of piezoelectric vibration energy harvesting system covered on curved beam with ABH.

3. Analysis of Harvesting Capacity of Piezoelectric Vibration Energy Harvesting System and Verification

3.1. Energy Harvesting Capacity Model. The basic principle used in the piezoelectric energy harvesting model is the piezoelectric effect. i.e., when the piezoelectric element deform due to the external force excitation, the opposite charge inside the piezoelectric element undergoes the polarization phenomenon. At this time, the two kinds of charges are shifted relative to each other, so as to gather the opposite charge on the relative surface of the piezoelectric element. The force-electrical coupling characteristics between the piezoelectric sheet and the ABH curved beam can be described by using piezoelectric intrinsic equations, which reflects the relationship between the stress-strain of piezoelectric elements and the electric potential shifting. The piezoelectric captive energy model adopted in this paper follows the abovementioned basic principles:

$$\begin{bmatrix} D \\ S \end{bmatrix} = \begin{bmatrix} d & \varepsilon^t \\ s^e & d^T \end{bmatrix}\begin{bmatrix} T \\ E \end{bmatrix}, \tag{8}$$

where D denotes the electric displacement, characterizing the positive piezoelectric effect; S denotes the strain, characterizing the inverse piezoelectric effect; d is the piezoelectric strain constant, s^e is the elastic flexibility constant of the piezoelectric element, T denotes the mechanical stress, and E denotes the generated electric field; ε^t is the dielectric constant of the piezoelectric material. After obtaining E, the voltage can be obtained from $V = Eh$, and the electric power can be obtained from $p = V^2/R$.

A model of curved beam with ABH is as shown in Figure 2. Figure 2(a) shows a 3D diagram of the model, in which the lower part is the curved beam with ABH and the upper part is the piezoelectric layer covered on the ABH part of curved beam, which form a piezoelectric vibrator. Width of the curved beam is 0.05 m. Figure 2(b) shows a 2D schematic of the model and the parameters. In Figure 2(b), R is radius, h_u is thickness, and a_0 is angle corresponding to arc length of curved beam, and translation springs P_1, P_2 and torsion springs Q_1, Q_2 are set at each end of the beam to simulate different boundary constraints. Next, an ABH of arc a_2 is embedded in the curved beam, where the thickness at the center of the ABH is h_0 (i.e. the truncated thickness), and the thickness of the ABH varies according to a power law ($h(s) = \varepsilon s^2$, s denotes the arc length of the neutral axis of the curved beam). The thickness of the piezoelectric layer covering the surface of the curved beam is h_2 and the harvesting circuit is formed by connecting a pure resistor R_L. The curved beam is considered as a cantilever beam structure with a fixed restraint at the left end (i.e., $P_2 = Q_2 = 0$ N/m), which is excited by a radial sinusoidal point force F whose amplitude is 5 N, causing tangential and radial displacements in the centerline of curved beam. In addition, the ABH weakens the stiffness of the curved beam, a problem that can be compensated by the inclusion of reinforcement, which is not discussed in this paper.

The structural characteristics of the ABH itself lead to the formation of phase accumulation and an increasing amplitude as the bending waves propagate to the tip. Then, high energy density in a localized region occurs, which theoretically provides the basis for achieving efficient vibration energy harvesting. In this paper, the finite element analysis is used for the numerical analysis. As the structural model is symmetrical and homogeneous in the width direction, and in order to improve the computational capacity, the analysis is completed in a 2D model. The FEA mesh is as shown in Figure 3. The influence of the wavelength compression effect (analyzed in detail in Section 4) causes the bending wavelength in the ABH region to decrease with increasing

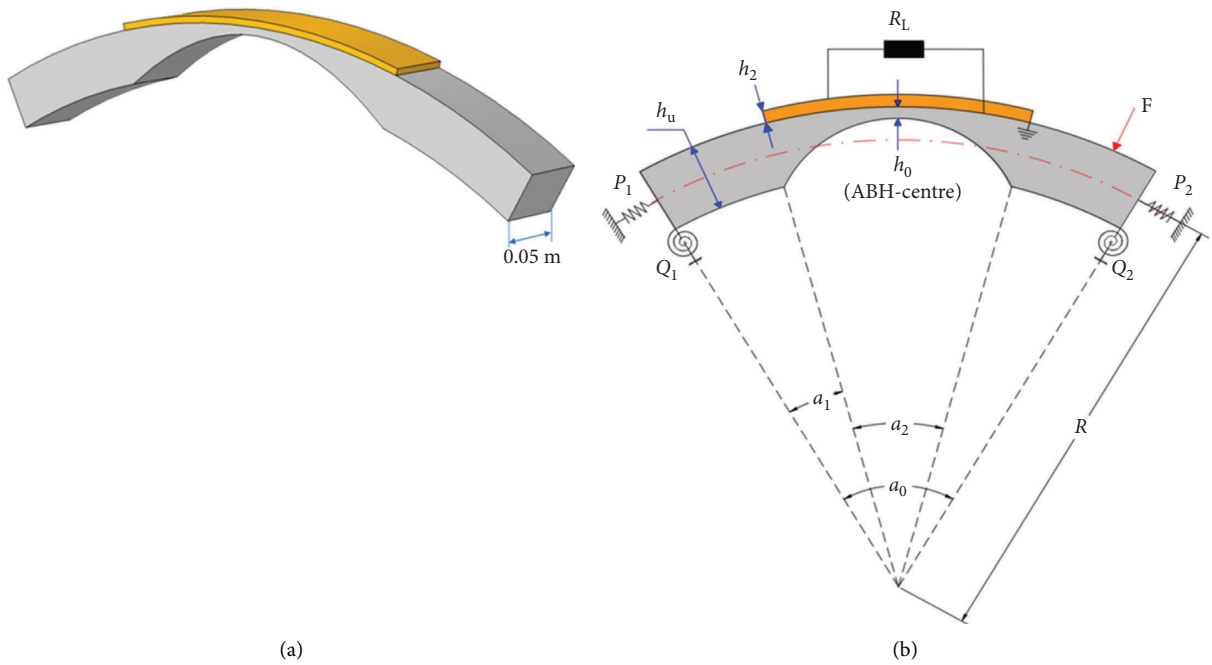

Figure 2: Schematic diagram of model structure. (a) 3D schematic diagram of ABH curved beam and piezoelectric sheet. (b) 2D schematic diagram of energy harvesting system and various parameters.

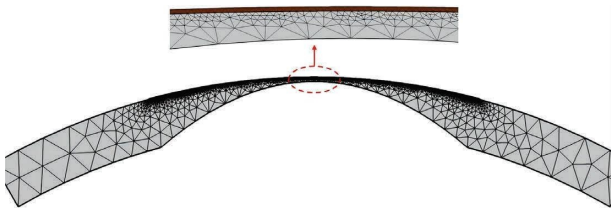

Figure 3: The mesh of ABH curved beam with a piezoelectric layer.

frequency, so in order to improve the accuracy of the results and adapt to the wavelength change, it is necessary to make sure that each wavelength contains at least 10 elements when meshing. For the model described in this paper, the frequency response of the structure from 0 Hz to 11500 Hz is analyzed mainly, when the wavelength corresponding to the maximum frequency value is 0.05 m. In this paper, the structure is delineated by free triangular solid elements. The stiffness of the connection surface of the piezoelectric layer and the ABH curved beam are not taken into account in finite element modeling, and both of them are directly connected by the way of common node to ensure the displacement continuity on the fitted surface of both of them. The displacements on the fitting surface are continuous. 4066 triangular solid elements are formed after meshing, including 781 triangular solid elements for the discretization of the piezoelectric layer. During the discretization process, 19,563 degrees of freedom are generated by the ABH bending beam and the piezoelectric layer. The size of each 10 elements in the ABH region is about 0.007 m, thus satisfying the requirement of including at least 10 elements in one wavelength.

Material and geometrical parameters of the structure are shown in Table 1, where ρ, E, μ are the material density, Young's modulus, and Poisson's ratio of the curved beam, respectively. C^E is the stiffness constant of the piezoelectric sheet; e is the piezoelectric stress constant; and ε^S denotes the dielectric constant.

3.2. Analysis of Energy Accumulation Effect of Curved Beams with ABH. In order to illustrate the energy distribution characteristics of the curved beam with ABH described in this paper, a radial point force excitation of amplitude 5 N is applied at the position shown in Figure 2(b). A fixed restraint is added at the left end of the beam (not covered with a piezoelectric layer) and the right end is free (i.e., set $P_1 = Q_1 = 10^{14}$ N/m and $P_2 = Q_2 = 0$ N/m). The material and geometry parameters are shown in Table 1. The frequency response range set in this paper is from 0 to 11500 Hz, which covers the first 10 orders of inherent frequency of the curved beam with ABH. RMS velocity response is shown in Figure 4 (the data are logarithmically processed in dB), and surface energy density of curved beam with ABH at different frequencies is shown in Figure 5.

From Figure 4, it can be seen that the velocity response of point 2 has a significant advantage over most of the frequency range, especially at the resonant frequencies, compared to points 1 and 3. Comparing point 1 with point 3, the velocity response of point 3 is slightly higher than that of point 1 in some frequency ranges, due to the location of point 3 closer to the excitation point.

Further, in order to visualize the energy distribution of the whole curved beam with ABH, the energy storage density (including kinetic energy, strain energy and dissipation

Table 1: Geometry and material parameters of ABH curved beam and piezoelectric layer.

Geometry parameters of ABH beam	Material parameters of ABH beam	Geometry parameters of PZT	Material parameters of PZT
$\varepsilon = 0.003$	$\rho = 7800\ \text{kg/m}^3$	$h_2 = 0.005$ m	$C^E = 1.27205 \times 10^{11}$ Pa
$h_u = 0.04$ m	$E = 2.1 \times 10^{11}$ Pa	$a_2 = \pi/6$	$e = -6.62281\ \text{C/m}^2$
$h_0 = 0.003$ m	$\mu = 0.3$		$\varepsilon^S = 1.2693 \times 10^{-8}$ F/m
$R = 0.5$ m			
$a_1 = \pi/12$			
$a_0 = \pi/3$			
P_1, P_2, Q_1, Q_2			

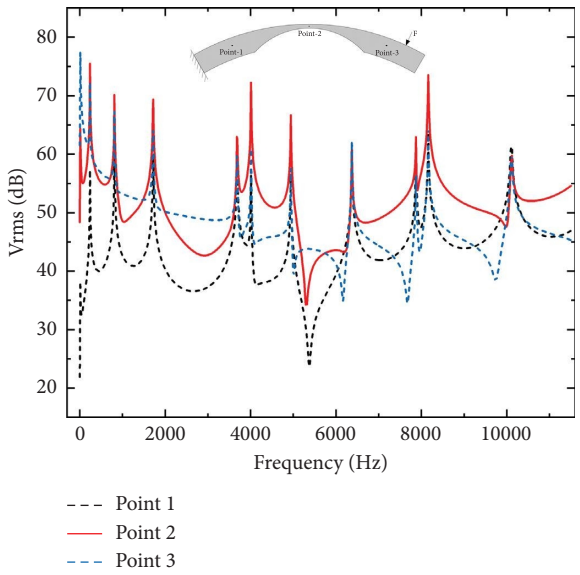

Figure 4: Root mean square velocity values of curved beam changing with frequency at several different positions.

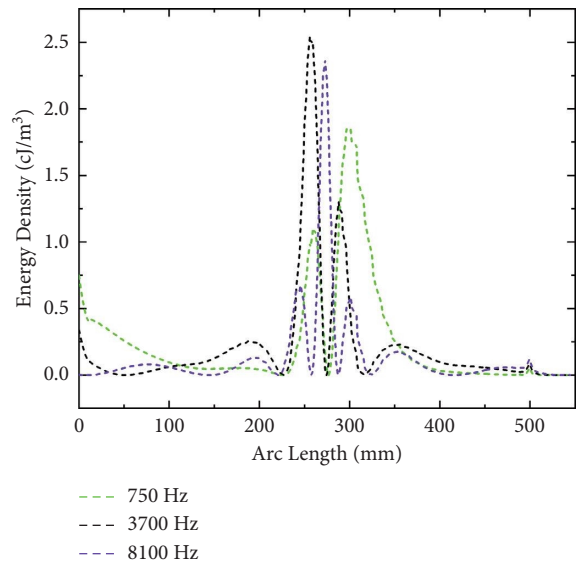

Figure 5: Surface energy density of curved beam changing with axis position at several different frequencies.

energy) is plotted along the arc length of the whole beam at different frequencies (750 Hz, 3700 Hz and 8100 Hz). It can be clearly seen from Figure 5 that the peak of the curve for each frequency is concentrated in the middle of the arc length, which is where the ABH region on the curved beam is located, and the energy density increases significantly closer to the center of the ABH. The above phenomenon indicates that embedding the ABH structure makes the fluctuation energy inside the curved beam highly aggregated in the ABH region, and the phenomenon also follows the basic principle of acoustic black hole effect. The above results are similar in the distribution characteristics of the vibration energy when compared with the conclusions of the paper [28–32] on the ABH straight beam structure, thus indicating that embedding the ABH structure on the curved beam has a positive effect on the enhancement of the energy aggregation effect. At the same time, it also provides the theoretical basis for the efficient harvesting of energy.

3.3. Verification of Energy Harvesting Capacity Model. In order to verify the energy harvesting capacity model and ensure that the results are reliable, an energy harvesting example in reference [25] is performed, and the electrical power is obtained if the frequency is 0~5000 Hz. The results from the model in this paper and the results from reference [25] are shown in Figure 6.

It can be seen from Figure 6, the results from energy harvesting capacity model built in this paper coincide to the results from reference [25].

3.4. Comparative Analysis of Energy Harvesting Capacity of Curved Beam with ABH and Uniform Curved Beam. In the previous section, an energy accumulation effect of the curved beam with ABH has been identified. Then, the energy harvesting capacity of piezoelectric vibration energy harvesting system covered on curved beam with ABH is investigated. In this section, the energy harvesting capacity of harvesting system covered on curved beams with ABH and uniform curved beams is compared and verified. The energy harvesting models for the uniform beam and curved beam with ABH are shown in Figure 7. The only difference between the two is that the curved beam with ABH is embedded with an ABH. All other geometry and material parameters remain the same for both. The piezoelectric

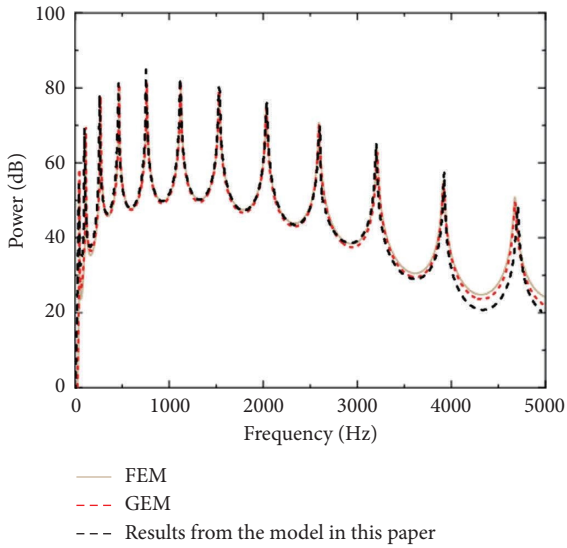

Figure 6: The electrical power from the model in this paper and from reference [25].

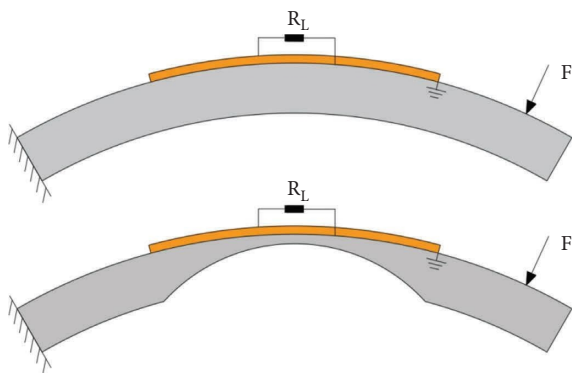

Figure 7: Energy harvesting model of uniform curved beam and curved beam with ABH.

material is PZT-5H, the piezoelectric sheet covers the entire ABH area, the resistance of R_L is 1000 Ω, and the rest parameters are referred to Table 1. The beam excited by the point force vibrates and the piezoelectric layer is driven by the piezoelectric effect to form an electric field, then outputs electrical energy through an external circuit. The output electric power of two kinds of beams is analyzed. In order to observe the difference more clearly, the data are processed by logarithm in this paper (10×1 g (velocity/10^{-13})) and use dB as the unit, finally obtaining the results as shown in Figure 8. In this paper, the electrical power values are mainly used to characterize the energy harvesting capability of the system.

In Figure 8, the black dashed and yellow solid lines represent the electrical power obtained from the curved beam with ABH and the uniform beam, respectively, in the range [0, 11500] Hz. From Figure 8, the following can be observed. On the one hand, the curved beam with ABH works better than the uniform beam over the entire frequency range. The data show that average power of the former is significantly about 23 dB higher than that of the latter. Therefore, it can be concluded that the ABH effect

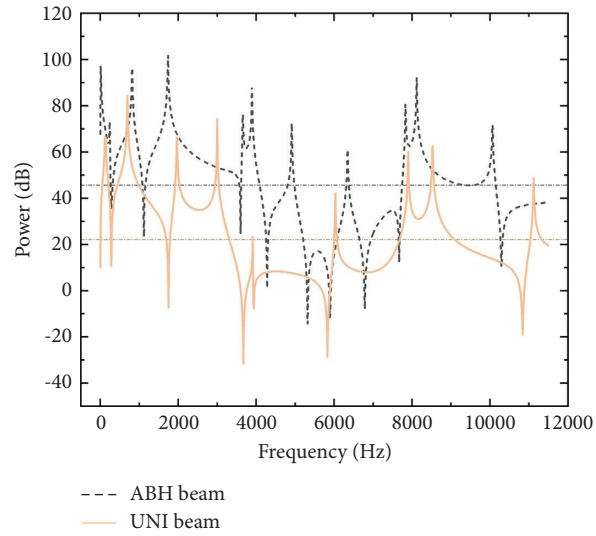

Figure 8: The electrical power harvested from uniform curved beam and curved beam with ABH.

plays a significant role in improving the vibration energy harvesting of curved beams. On the other hand, the curved beam with ABH maintains good energy harvesting performance in the full frequency range, but its performance decays as the excitation frequency increases. The power value starts to weaken above 2000 Hz compared to the lower frequency range, resulting in a significantly weaker harvesting in the middle and high frequency range than in the lower frequency range. This, in turn, is caused by wavelength compression within the structure, about which more will be said in the following. It can therefore be concluded that the ABH effect has the potential to enhance the energy harvesting performance of the curved beam, but that the design layout of the piezoelectric cell also has an important influence on this.

4. Key Influencing Parameters of Energy Harvesting Capacity

In the previous section, it is found that wavelength compression has a certain influence on the energy harvesting performance of the structure, and this occurs in the ABH region of the curved beam, as shown by the fact that the wavelength of the bending wave inside the ABH decreases with increasing external excitation frequency. Based on the Euler–Bernoulli beam theory, the local wave number of the bending wave inside the variable-thickness beam is obtained according to literature [38] as follows:

$$k = \left[\frac{12\rho\omega^2\left(1-\mu^2\right)}{Eh^2(s)}\right], \tag{9}$$

where ρ is the material density, μ and E are Poisson's ratio and Young's modulus, respectively, $h(s)$ is the local thickness of the curved beam, ω is the angular frequency, and the wave speed c can be expressed by the wave number k as $c = \omega/k$

$$c = (\omega h)^{1/2}\left[\frac{E}{12\rho(1-\mu^2)}\right]^{1/4}. \quad (10)$$

Using $c = 2\pi\omega\lambda$, the relationship between the wave speed c and the wavelength λ, the wavelength can be expressed as follows:

$$\lambda = 2\pi\left(\frac{h}{\omega}\right)^{1/2}\left[\frac{E}{12\rho(1-\mu^2)}\right]^{1/4}. \quad (11)$$

From equation (11), it can be found that when other parameters are determined, the relationship between wavelength and frequency is consistent with the phenomenon described above. In this paper, when the system is excited to produce a vibrational response, the piezoelectric cell is polarized in different directions by stretching and compression, resulting in charges of opposite electrode nature on the surface. If the size of the piezoelectric sheet exceeds half a wavelength at this point, the anisotropic charges will be cancelled out, thus weakening the energy harvesting performance of the structure to some extent, which is also consistent with the situation described by Ji et al. in the case of straight beams in reference [17]. Therefore, for piezoelectric sensors, the size design should be combined with the wavelength factor.

4.1. Influence of Layout of the Piezoelectric Sheet. The wavelength compression phenomenon explains the query raised in Section 3 of this paper: when a whole piezoelectric sheet is covered in the ABH region, the energy harvesting capacity in the middle and high frequency bands is lower than in the low frequency bands. In this subsection, the negative effect caused by the wavelength compression phenomenon is overcome by matching the relationship between piezoelectric cell size and wavelength. When the frequency value is set to the maximum value of the frequency response (11500 Hz), the material parameters are substituted in equation (10), the minimum wavelength at the center of the ABH region is obtained as 0.05 m. When the piezoelectric sheet is divided into 10 cells as shown in Figure 9, the arc length of each piezoelectric cell is 0.025 m, thus satisfying the requirement that the size of a single piezoelectric cell does not exceed half a wavelength. The contact surface between the piezoelectric cell and the upper surface of the curved beam with ABH is set to zero potential. The upper surface of the piezoelectric cell is connected to a collection terminal. While a resistor is connected to each piezoelectric cell (here, all 10 resistors have a resistance of 1000 Ω) as an external load to complete the energy harvesting.

After recalculation, the electrical power results for the new configuration are obtained. Figure 10 describes the results for three cases: 10PZT-ABH (energy harvesting system combined by 10 piezoelectric cells covered on curved beam with ABH), 1 PZT-ABH (energy harvesting system combined by one piezoelectric cell covered on curved beam with ABH), and 1PZT-UNI (energy harvesting system combined by one piezoelectric cell covered on uniform curved beam). All of the single piezoelectric cells described above have a load resistance of 1000 Ω. In order to better

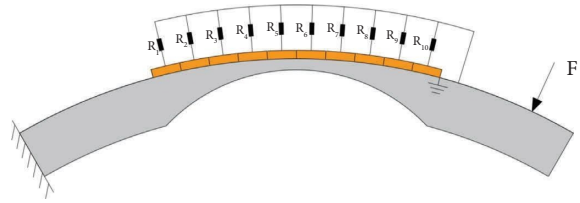

Figure 9: Diagram of dividing the piezoelectric sheet into 10 cells.

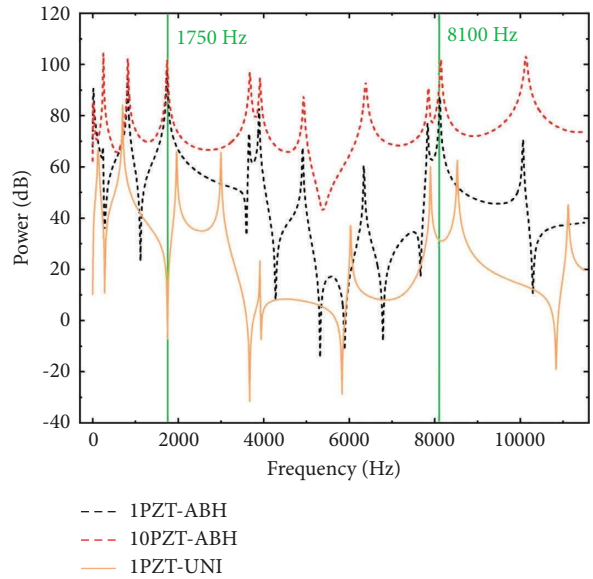

Figure 10: The electrical power harvested from 10PZT-curved beam with ABH, 1PZT-curved beam with ABH, and 1PZT-uniform curved beam.

visualize the outstanding contribution made by the arrayed piezoelectric cells, the frequency range is divided into three intervals, low (0~1750 Hz), medium (1750~8100 Hz), and high (8100~11500 Hz), according to the trend of the result in the Figure 10. Then, the average power in each interval is calculated, and the results are shown in Figure 11. Next, to further validate the theoretical analysis of the wavelength compression effect, the energy harvesting effects of different numbers of piezoelectric cells (1PZT, 3PZT, 5PZT, and 10PZT) covered on the curved beam with ABH are compared in Figure 12.

In Figure 10, the results show that splitting the piezoelectric sheet into 10 cells significantly enhances the energy harvesting capacity of the structure in the mid to high frequency band (red dashed line in the Figure).

From Figure 11, the following phenomena are easily noticeable: on the one hand, the average power of the arrayed PZT layout is 29.1 dB and 33.9 dB higher in the mid- and high-frequency intervals respectively than the single PZT layout approach, a value that is approximately three times higher (11.3 dB) than in the low frequency band. This result is also in line with what we would expect from an array layout. On the other hand, over the entire frequency range, the average power value of the array layout is increased by 60.8%

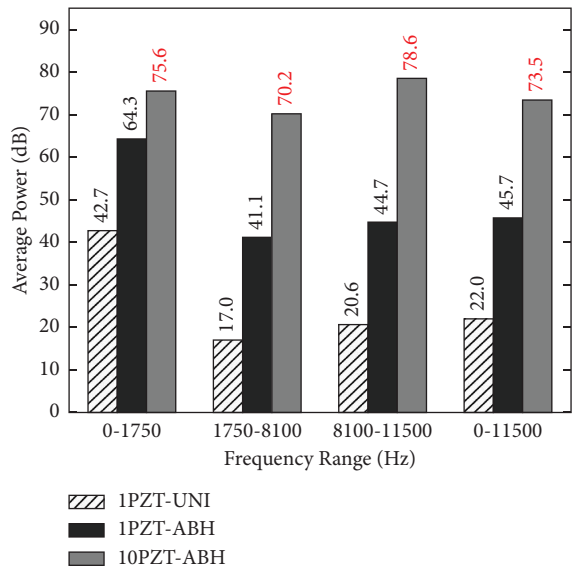

Figure 11: Average harvested power of 10PZT-curved beam with ABH, 1PZT-curved beam with ABH, and 1PZT-uniform curved beam.

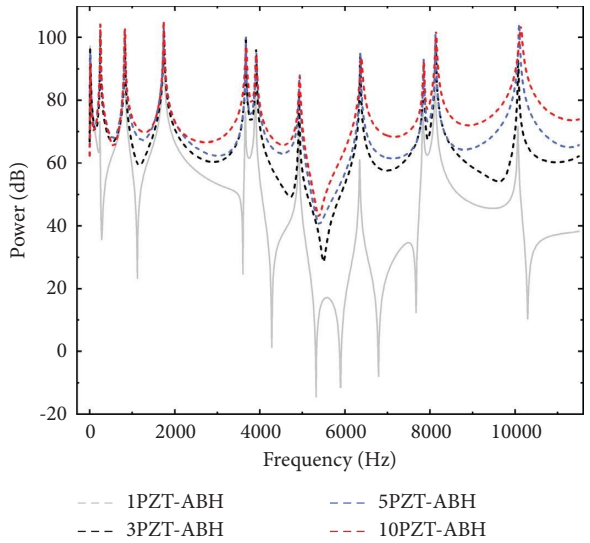

Figure 12: The electrical power harvested from the energy harvesting system combined by different numbers of a piezoelectric cell.

compared to a single piezoelectrical layout for curved beams with ABH, and by a significant 223.8% compared to a single patch layout for uniform curved beams.

The results in Figure 12 show that the splitting of the piezoelectrical sheet into 10 cells gives better results than several other solutions, regardless of the frequency interval. It can therefore be concluded that the array layout of piezoelectric cells can effectively improve the energy harvesting effect of curved beams with ABH in the mid to high frequency range, overcoming the negative effects of wavelength compression, and also providing a solution for broadband vibration energy harvesting of the structure.

Furthermore, in order to verify the theoretical analysis of the wavelength compression effect above, the maximum value of the frequency response is set to 5000 Hz, and the minimum wavelength at the center of ABH can be calculated from equation (10) as 0.09 m. At this time, the arc length of each piezoelectric piece is 0.043 m when the piezoelectric piece is divided into 6 pieces, which meets the requirement of less than half wavelength. At the same time, the power values of 1 PZT, 6 PZT, and 10 PZT in 0~5000 Hz are plotted in Figure 13, respectively.

In the Figure 13, since the maximum frequency value is 5000 Hz, according to the wavelength compression effect that the piezoelectric sheet size should be less than half the wavelength, the piezoelectric sheet is divided into 6 pieces. The information from the Figure 13 shows that the power value after dividing the piezoelectric sheet is significantly better than that of one piezoelectric sheet. Meanwhile, the values and trends of the two curves for dividing the piezoelectric sheet into 6 and 10 pieces are the same throughout the frequency interval. Therefore, it can be explained that in order to overcome the adverse effects of wavelength compression phenomenon, it is sufficient to meet the requirement that the piezoelectric sheet size is less than half wavelength when dividing the piezoelectric sheet.

4.2. Influence of Resistance of a Resistor. A resistor is part of an energy harvesting circuit, so it is necessary to discuss in detail the effect of different resistance values on energy harvesting capacity. In this section, for curved beam with ABH, with different resistances, the power of energy harvesting system combined by 1 piezoelectric cell is computed. The results are shown in Figure 14. In addition, the power of energy harvesting system combined by 10 piezoelectric sheets is computed; the results are shown in Figure 15. For an energy harvesting system combined by 10 piezoelectric cells, in order to find best resistance at every frequency, electrical power at different resistances (from 102 Ω to 104 Ω in steps of 100.2 Ω) and different frequencies is computed, and the results are shown in Figure 16.

The results show that the load resistance is an important parameter affecting the electrical power. From Figure 14, where the 3 curves correspond to different resistance values (1 kΩ, 5 kΩ and 10 kΩ), it is clear that the larger resistance value is better results if the frequency is less than 100 Hz, (observe the miniature plot in the bottom left corner). In contrast, when the frequency exceeds 100 Hz, resistors with a resistance value of 1 kΩ are always in the lead.

From Figure 15, a similar phenomenon can be found, with the 10 kΩ resistor producing significantly better power values than the other resistances in the 0 to 1000 Hz range, while the 1 kΩ resistor has a better performance as the frequency gradually increases. In Figure 16, the black curve indicates the resistance value corresponding to the best power at different frequencies. It can be noticed that for lower frequencies the optimum resistance value is higher, while as the frequency continues to increase, the optimum resistance value gradually converges to a smaller value. This phenomenon may be related to the electric circuit characteristics. Piezoelectric sheets can be equivalent to voltage sources and capacitors, forming RC series circuits together with resistors. Due to the resistor being the output component in this case, the RC circuit is a high-

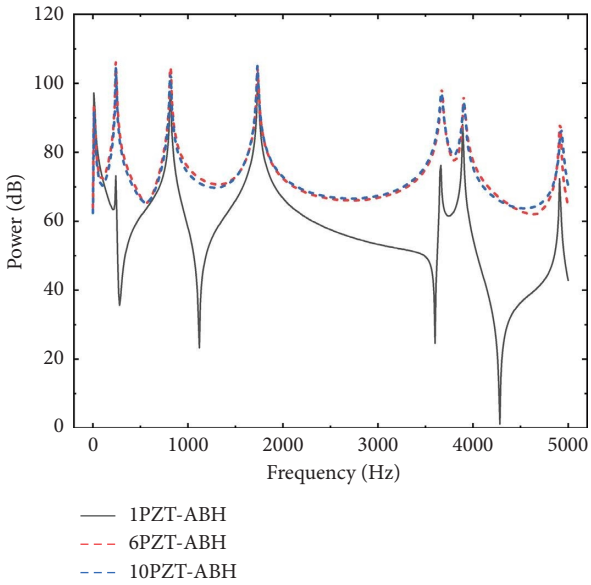

Figure 13: Power of ABH curved beam in 0~5000 Hz with different piezoelectric sheet layouts.

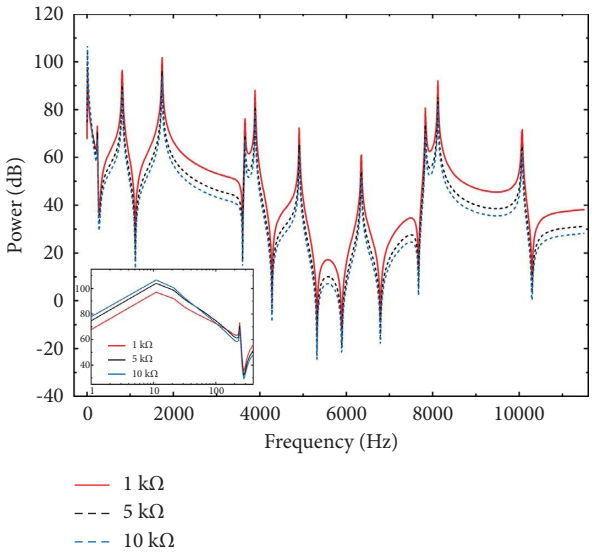

Figure 14: Harvested power corresponding to different resistance values for energy harvesting system combined by 1 piezoelectric cell.

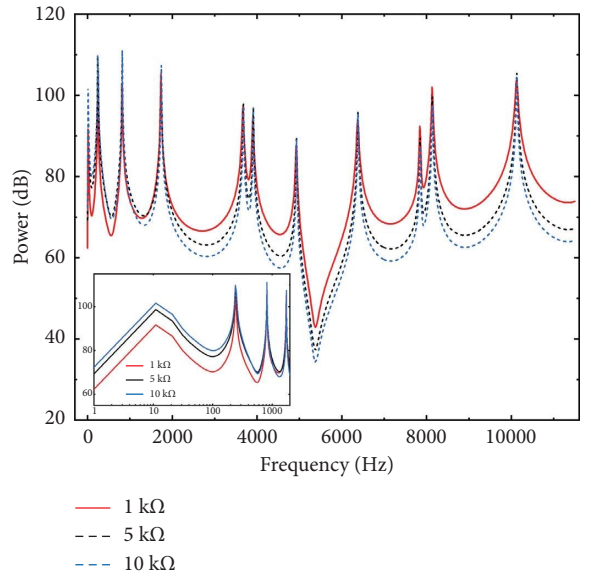

Figure 15: Harvested power corresponding to different resistance values for energy harvesting system combined by 10 piezoelectric cells.

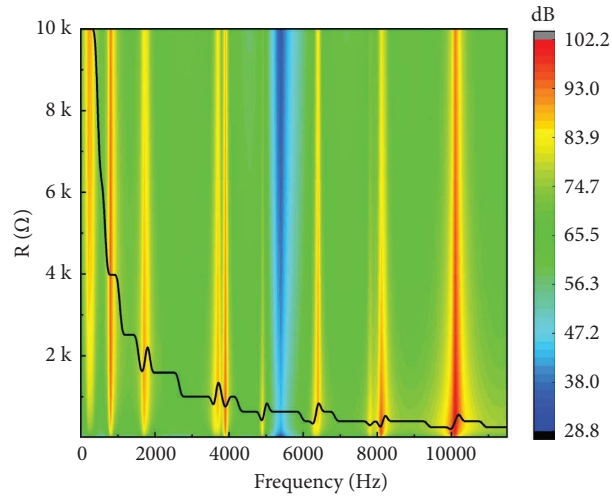

Figure 16: Electrical power changing with load resistance and frequency for energy harvesting system combined by 10 piezoelectric cells.

frequency pass circuit. The critical frequency ($\omega_0 = 1/RC$) is a key parameter for a RC circuit. If the frequency is greater than the critical frequency, the output voltage does not change significantly with the frequency. If the frequency is less than the critical frequency, the output voltage significantly decreases [39]. Reducing the critical frequency can increase the output voltage and increase the harvested power. The critical frequency can be reduced by increasing the R value. Therefore, the optimal resistance value in the low frequency range is relatively large.

It can therefore be concluded that the value of the load resistance has a significant effect on the energy harvesting performance. The selection of the resistance value should focus on the frequency environment of the system and should be matched to different resistance values in order to improve the energy harvesting capability.

4.3. Influence of Material and Thickness of Piezoelectric Layer. In addition to the influence of the layout of the piezoelectric sheet and the load resistance, the parameters of piezoelectric layer are also important factor that effect on the energy harvesting capacity. The material and geometric size of piezoelectric layer are the key factors. This section focuses on the effect of different piezoelectric material types and geometrical thicknesses on the energy harvesting capacity.

Piezoelectric materials mainly include organic piezoelectric materials, inorganic piezoelectric materials and composite piezoelectric materials [1]. Among them, organic

piezoelectric materials are also known as piezoelectric polymers and common inorganic piezoelectric materials are piezoelectric crystals and piezoelectric ceramics. In this section, three materials, quartz crystal (piezoelectric crystal), PZT-5H (piezoelectric ceramic), and PVDF (piezoelectric polymer), were chosen for comparison. The harvested power values for the three materials in the [0, 11500] Hz range is shown in Figure 17.

From Figure 17, it is clear that the energy harvesting capacity of PZT-5H is significantly better than the other two, due to the high dielectric constant and piezoelectric properties of the piezoelectric ceramics. The quartz crystal has a higher mechanical quality factor and the PVDF is more flexible than the PZT-5H. It is important to note that with the emergence of new piezoelectric composites that combine various advantages, there will be a positive impact on the energy harvesting capacity of curved beam with ABH.

Also, in order to investigate the effect of geometrical thicknesses on the harvesting performance, the electrical power corresponding to four different thicknesses (0.5 mm, 1.0 mm, 1.5 mm, and 2.0 mm) of piezoelectric layer are compared and shown in Figure 18. The average power values for the four thicknesses at different frequency ranges are shown in Figure 19.

From Figure 18, it can be observed that the four curves do not show more significant differences in the 0 to 6500 Hz range, except at the resonance peak near 1000 Hz (where the power of the 1.0 mm PZT is significantly higher by about 14.5 dB and 4.5 dB compared to the other thicknesses). The effect of the thickness factor is highlighted when the frequency exceeds 6500 Hz, where the 2 mm thick piezoelectric sheet has a better effect than the other sizes. From Figure 19, it is shown that the increase in thickness has a more pronounced effect on the power increase when the frequency is within 6500–11500 Hz compared to 0–6500 Hz, with 1.5 mm PZT and 2.0 mm PZT showing an average power increase of 7.6% and 8.7%, respectively, compared to 0.5 mm PZT, while this value is 5.0% and 5.4%. It can therefore be judged that the increase in thickness of piezoelectric layer is limited in terms of power improvement in the low frequency range and throughout the frequency range, while for the higher frequency range this improvement is more pronounced.

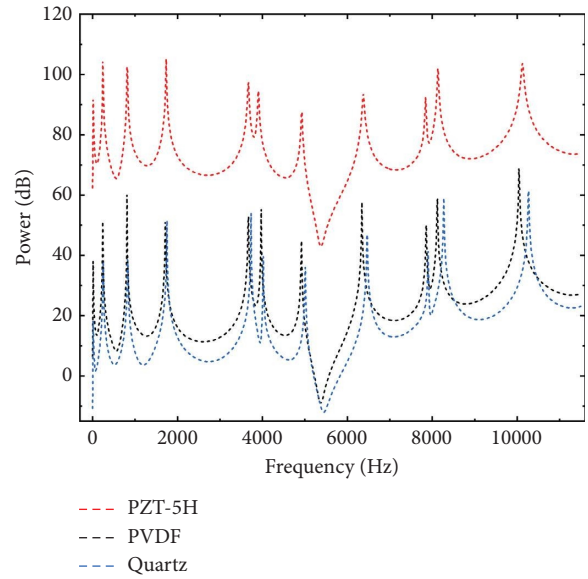

Figure 17: Energy harvesting capacity of different piezoelectric materials.

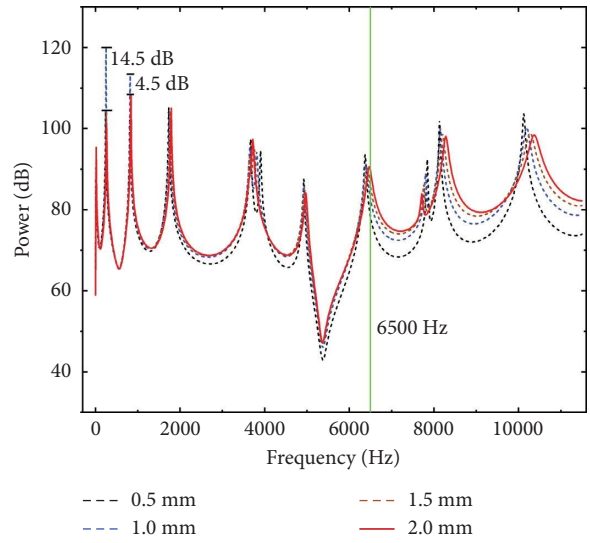

Figure 18: Energy harvesting capacity corresponding to four piezoelectric thicknesses.

4.4. Influence of Curvature. Curvature should be taken into account as an important structural parameter. In this section, five different curvatures ($k_1 = 1/470$, $k_2 = 1/480$, $k_3 = 1/490$, $k_4 = 1/500$, $k_5 \longrightarrow 0$) of curved beams with ABH are considered, where a straight beam is used instead of the case when $k_5 \longrightarrow 0$. Except for the difference in curvature, the other parameters are identical. As a comparison, the paper focuses on the effect of curvature on the energy harvesting capacity. The electrical power harvested from the above-mentioned beams in the range 0 to 11500 Hz is shown in Figure 20.

From Figure 20, it can be seen that there is a relative shift in the position of the resonance peaks for the different curves. Below about 5000 Hz, the power from straight beams is high than that from others, so it can be concluded that the energy harvesting advantage of the straight beams being mainly in the low- to mid-frequency range. Looking at the curve corresponding to the curvature k_5 shows that the values corresponding to this curve lag behind the other curves in the frequency axis when the frequency exceeds around 6500 Hz. Therefore, we split the frequency range into two parts through taking 6500 Hz as the boundary and calculated their average power separately, as shown in Figure 21.

From Figure 21, it is shown that the average power of the straight ABH beam is higher than the other curved beams within 0 to 6500 Hz. The situation changes when the frequency exceeds 6500 Hz, and the overall average power value for the other ABH curved beams (k_1–k_4) is 76.77 dB, which is an increase of about 12.76% compared to the straight beams. The

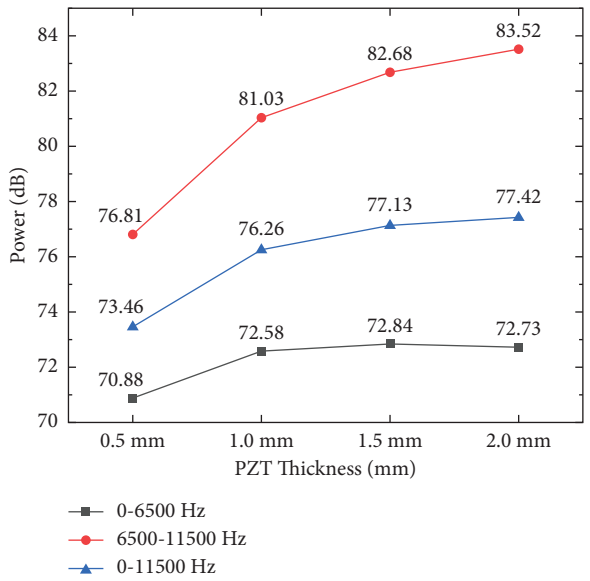

Figure 19: Average power of energy harvesting capacity in different frequency ranges corresponding to four piezoelectric thicknesses.

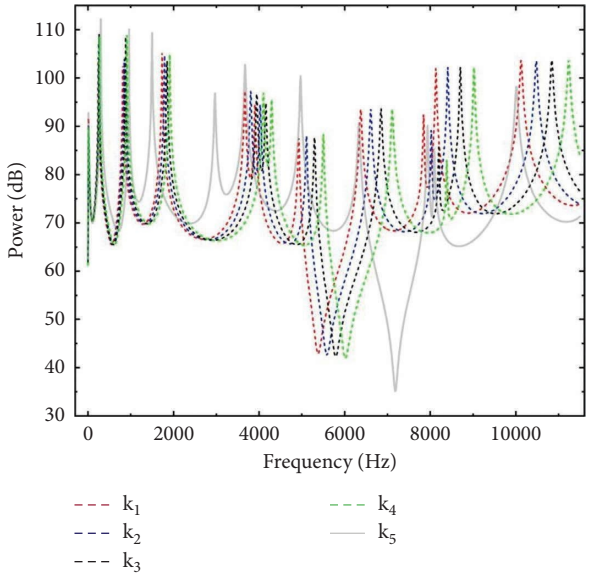

Figure 20: Harvesting capacity corresponding to curved beam with ABH at different curvatures.

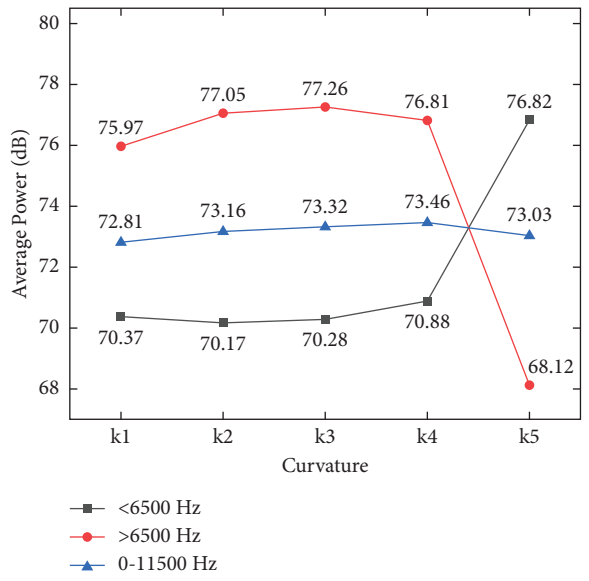

Figure 21: Average power of different curvatures in different frequency ranges.

difference between the average power of all curved beams is smaller in the full frequency range. Thus, we can find that the curvature causes a relative shift in the resonance peak of the structure. Compared to straight beams, curvature somewhat weakens the energy harvesting performance of the structure in the low and medium frequency range, while also enhancing the energy harvesting capability of the structure in the high frequency range.

5. Discussion

In this paper, a curved beam with ABH and a vibration energy harvesting system is constituted by attaching piezoelectric layer to the upper surface of the ABH region. The vibration response characteristics of a curved beam with ABH and energy harvesting effect of vibration energy harvesting system in a wide frequency range are analyzed to reveal the potential of the structure in energy harvesting. The energy harvesting capacity of the curved beam with ABH is compared with that of a uniform curved beam under the same conditions, and the curved beam with ABH achieves satisfactory results. At the same time, the reason for the weakened energy harvesting performance of the curved beam with ABH in the high frequency range is found by analyzing the wavelength compression effect. Then, an array of piezoelectric cells was used, to solve the problem and achieving the desired goal. In the work that follows, several important factors are discussed in detail. The data show that the external load resistance has a significant effect on the energy harvesting capacity, and larger resistance values give better results in the lower frequency range, while the opposite is true in the high frequency range. It should be noted that the load resistance value of the array should also be matched to the actual frequency environment in which it is used to achieve optimum energy harvesting. Then, the influence of different piezoelectric sheet materials and geometrical thicknesses on the energy harvesting by the system is discussed. The results show that the piezoelectric material has an important influence on the electrical power value. A piezoelectric material with better piezoelectric properties and a higher dielectric constant can effectively improve the harvesting performance of the system. For the piezoelectric sheet thickness, the variation in thickness is more sensitive to the effect in the high frequency interval. In the high frequency range, the energy harvesting capacity increases to a certain extent as the thickness increases. In addition, the effect of curvature on power is analyzed for straight beams with ABH ($k \longrightarrow 0$), and the effect of curvature is mainly occurs in the high frequency range. In the low frequency range, the curved beam with ABH has a slightly lower

harvesting performance than the straight ABH beam, while in the high frequency range, the curved beam with ABH shows better results.

Finally, it is also important to emphasize that different forms of external circuitry can also have an effect on the energy harvesting capacity to some extent. As pure resistance is used instead of load in this paper, the results presented do not represent the optimum energy conversion capability of the system. In the meantime, the effect of the curved beam with ABH on the structural strength of the curved beam will be investigated in detail in subsequent work.

Data Availability

The data used to support the findings of this study are included within the article.

Conflicts of Interest

The authors declare that there are no conflicts of interest regarding the publication of this paper.

Acknowledgments

This research was funded by National Natural Science Foundation of China (51305330), Shaanxi Province Qinchuangyuan "Scientists + Engineers" Team Construction (2022KXJ032), and Special Scientific Research Foundation of Department of Education from Shaanxi Province (15JK1438).

References

[1] M. A. Mironov, "Propagation of a flexural wave in a plate whose thickness decreases smoothly to zero in a finite interval," *Soviet Physics Acoustics-USSR*, vol. 34, no. 3, pp. 318-319, 1988.

[2] V. V. Krylov and A. L. Shuvalov, "Propagation of localised flexural vibrations along plate edges described by a power law," *Proceedings of the Institute of Acoustics*, vol. 22, no. 2, pp. 263–270, 2000.

[3] V. Krylov and F. Tilman, "Acoustic black holes for flexural waves as effective vibration dampers," *Journal of Sound and Vibration*, vol. 274, no. 3-5, pp. 605–619, 2004.

[4] X. Du, D. Huang, and J. Zhang, "Dynamic property investigation of sandwich acoustic black hole beam with clamped-free boundary condition," *Shock and Vibration*, vol. 2019, Article ID 6708138, 14 pages, 2019.

[5] Q. Fu, X. Du, J. Wu, and J. Zhang, "Dynamic property investigation of segmented acoustic black hole beam with different power-law thicknesses," *Smart Materials and Structures*, vol. 305, Article ID 055001, 2021.

[6] L. Tang and L. Cheng, "Periodic plates with tunneled Acoustic-Black-Holes for directional band gap generation," *Mechanical Systems and Signal Processing*, vol. 133, Article ID 106257, 2019.

[7] L. Ma and L. Cheng, "Sound radiation and transonic boundaries of a plate with an acoustic black hole," *Journal of the Acoustical Society of America*, vol. 145, no. 1, pp. 164–172, 2019.

[8] X. Wang, H. Ji, J. Qiu, and L. Cheng, "Wavenumber domain analyses of vibro-acoustic decoupling and noise attenuation in a plate- cavity system enclosed by an acoustic black hole plate," *Journal of the Acoustical Society of America*, vol. 146, no. 1, pp. 72–84, 2019.

[9] H. X. Ji, J. Wang, L. Qiu, Y. Cheng, and C. Zhang, "Noise reduction inside a cavity coupled to a flexible plate with embedded 2-D acoustic black holes," *Journal of Sound and Vibration*, vol. 455, pp. 324–338, 2019.

[10] X. Li and Q. Ding, "Sound radiation of a beam with a wedge-shaped edge embedding acoustic black hole feature," *Journal of Sound and Vibration*, vol. 439, pp. 287–299, 2019.

[11] L. Tang and L. Cheng, "Impaired sound radiation in plates with periodic tunneled Acoustic Black Holes," *Mechanical Systems and Signal Processing*, vol. 135, Article ID 106410, 2020.

[12] R. Guillaume, J. Y. Lee, W. Jeon, P. Adrien, and F. Gautier, "On the control of the absorption of an Acoustic Black Hole by using attached point supports," *Journal of Sound and Vibration*, vol. 548, 2023.

[13] Y. Bao, X. Liu, Z. Yao, Y. Shan, and T. He, "Research on vibration absorption and isolation characteristics of periodic acoustic black hole beam resonators and their enhancement," *International Journal of Applied Mechanics*, vol. 15, no. 1, 2023.

[14] S. Gao, Z. Tao, Y. Li, and F. Pang, "Application research of acoustic black hole in floating raft vibration isolation system," *Reviews on Advanced Materials Science*, vol. 61, no. 1, pp. 888–900, 2022.

[15] R. Zhu, Y. Liu, B. Navya, Z. Qin, and F. Chu, "Vibration attenuation of rotating disks via acoustic black holes," *International Journal of Mechanical Sciences*, vol. 242, 2023.

[16] L. Zhao, S. Conlon, and F. Semperlotti, "Broadband energy harvesting using acoustic black hole structural tailoring," *Smart Materials and Structures*, vol. 23, no. 6, Article ID 065021, 2014.

[17] H. Ji, Y. Liang, J. Qiu, L. Cheng, and Y. Wu, "Enhancement of vibration based energy harvesting using compound acoustic black holes," *Mechanical Systems and Signal Processing*, vol. 132, pp. 441–456, 2019.

[18] C. Yang, Y. Yuan, H. Wang, Y. Tang, and J. Gui, "Research on vibration energy harvester based on two-dimensional acoustic black hole," *Micromachines*, vol. 14, no. 3, p. 538, 2023.

[19] H. Zhu and F. Semperlotti, "Two-dimensional structure-embedded acoustic lenses based on periodic acoustic black holes," *Journal of Applied Physics*, vol. 122, no. 6, Article ID 065104, 2017.

[20] S. Yan, A. M. Lomonosov, and Z. Shen, "Numerical and experimental study of Lamb wave propagation in a two-dimensional acoustic black hole," *Journal of Applied Physics*, vol. 119, no. 21, Article ID 214902, 2016.

[21] S. S. Ganti, T.-W. Liu, and F. Semperlotti, "Topological edge states in phononic plates with embedded acoustic black holes," *Journal of Sound and Vibration*, vol. 466, Article ID 115060, 2020.

[22] Y. Mi and H. Zheng, "Enhancement of acoustic black hole effect in beams using shunted piezo-electric patch," *INTER-NOISE and NOISE-CON Congress and Conference Proceedings*, vol. 259, pp. 242–248, 2019.

[23] L. Zhao, S. C. Conlon, and F. Semperlotti, "An experimental study of vibration based energy harvesting in dynamically tailored structures with embedded acoustic black holes," *Smart Materials and Structures*, vol. 24, no. 6, Article ID 065039, 2015.

[24] L. Zhang, G. Kerschen, and L. Cheng, "Electromechanical coupling and energy conversion in a PZT-coated acoustic

black hole beam," *International Journal of Applied Mechanics*, vol. 12, no. 8, Article ID 2050095, 2020.

[25] J. Deng, O. Guasch, L. Zheng, T. Song, and Y. Cao, "Semi-analytical model of an acoustic black hole piezoelectric bimorph cantilever for energy harvesting," *Journal of Sound and Vibration*, vol. 494, Article ID 115790, 2021.

[26] H. Li, O. Doaré, C. Touzé, and P. Adrien, "Energy harvesting efficiency of unimorph piezoelectric acoustic black hole cantilever shunted by resistive and inductive circuits," *International Journal of Solids and Structures*, vol. 238, 2023.

[27] Y. Qin, G. Han, and Y. Mao, "Two-dimensional Eulerian-exponential-law acoustic black hole structure for energy harvesting," *IEEE Sensors Journal*, vol. 23, no. 11, pp. 11762–11773, 2023.

[28] Z. Zhang, H. Wang, C. Yang, H. Sun, and Y. Yuan, "Vibration energy harvester based on bilateral periodic one-dimensional acoustic black hole," *Applied Sciences*, vol. 13, no. 11, p. 6423, 2023.

[29] D. Xiong, J. Liang, Y. Qiao, and S. Qi, "Enhanced acoustic black hole energy harvesters with multipiezoelectric array designs," *Applied Physics Express*, vol. 16, no. 4, Article ID 045502, 2023.

[30] X. Chen, J. Zhao, J. Deng, Y. Jing, H. Pu, and J. Luo, "Low-frequency enhancement of acoustic black holes via negative stiffness supporting," *International Journal of Mechanical Sciences*, p. 241, 2023.

[31] C. Yang, T. Ye, M. Qiu, Z. Zhai, and P. Hu, "A semi- analytical framework for comprehensive vibration analysis of segment-coupled plates with embedded acoustic black holes," *Thin-Walled Structures*, vol. 184, 2023.

[32] Y. Zhen, T. Gu, and Y. Tang, "Aeroelastic analysis and active control of one- dimensional acoustic black hole structures in supersonic airflow," *Engineering Analysis with Boundary Elements*, vol. 147, 2023.

[33] B. Han, H. Ji, L. Cheng, W. Huang, and J. Qiu, "Attenuation band splitting in a finite plate strip with two-dimensional acoustic black holes," *Journal of Sound and Vibration*, vol. 546, 2023.

[34] Q. Fu, J. Wu, C. Yu, X. Du, N. Zhang, and J. Zhang, "Parametric studies and optimal design of the exponents collocation of a segmented acoustic black hole beam," *Applied Acoustics*, vol. 200, 2022.

[35] J. Deng, O. Guasch, L. Maxit, and L. Zheng, "Annular acoustic black holes to reduce propagative Bloch-Floquet flexural waves in periodically supported cylindrical shells," *INTER-NOISE and NOISE-CON Congress and Conference Proceedings*, vol. 259, 2010.

[36] J. Deng, O. Guasch, and L. Zheng, "A semi-analytical method for characterizing vibrations in circular beams with embedded acoustic black holes," *Journal of Sound and Vibration*, vol. 476, Article ID 115307, 2020.

[37] J. Deng, O. Guasch, L. Maxit, and L. Zheng, "Vibration of cylindrical shells with embedded annular acoustic black holes using the Rayleigh-Ritz method with Gaussian basis functions," *Mechanical Systems and Signal Processing*, vol. 150, Article ID 107225, 2021.

[38] J. Deng, O. Guasch, L. Maxit, and L. Zheng, "Annular acoustic black holes to reduce sound radiation from cylindrical shells," *Mechanical Systems and Signal Processing*, vol. 158, Article ID 107722, 2021.

[39] Z. H. Qin, *Electrical Engineering*, Higher Education Press, Beijing, China, 1991.